Magnetic properties and giant magnetoresistance of melt-spun granular Cu_{100-x}-Co_x alloys

P. Allia

Dipartimento di Fisica, Politecnico di Torino, Corso Duca degli Abruzzi 24, I-10129 Torino, Italy
and Istituto Nazionale di Fisica della Materia, Section of Torino Politecnico, I-10129 Torino, Italy

M. Knobel

Instituto de Fisica "Gleb Wataghin," Universidade Estadual de Campinas, Caixa Postal 6165, 13083-970 Campinas, São Paulo, Brazil

P. Tiberto and F. Vinai

IEN Galileo Ferraris, Corso Massimo d'Azeglio 42, I-10125 Torino, Italy
and Istituto Nazionale di Fisica della Materia, Section of Torino Politecnico, I-10129 Torino, Italy

Room-temperature measurements of magnetization and giant magnetoresistance were performed on rapidly solidified granular $Cu_{100-x}Co_x$ systems ($x=5,10,15$). The magnetoresistance of melt-spun $Cu_{100-x}Co_x$ ribbons was enhanced either by suitable furnace annealings or by exploiting the dc Joule-heating technique in the attempt of precipitating smaller magnetic particles. The particle-size distribution, the particle density, and mean distance are obtained for all compositions and heat treatments through a suitable analysis of the magnetic behavior of samples. The magnetoresistance is plotted as a function of the reduced magnetization, and a significant deviation from the quadratic behavior predicted by the independent-moment approach is observed at low fields. A simple theory taking explicitly into account the correlation existing among the magnetic particles is proposed. A general expression for the magnetoresistance in granular magnetic systems is obtained, and shown to accurately fit all the experimental curves, indicating that this effect is basically determined by the ratios between two distinct correlation ranges for the magnetic-moment fluctuations and the electronic mean free path.

I. INTRODUCTION

The so-called granular magnetic systems, consisting of nanometer-sized particles of a magnetic metal (e.g., Fe, Co) dispersed in a nonmagnetic metallic matrix (e.g., Ag, Cu), have been extensively investigated in the past few years. One of the major causes of this growing interest was the discovery of the occurrence of an effect of giant magnetoresistance (GMR) in such materials, made simultaneously by Berkowitz et al.[1] and Xiao et al.[2] The GMR effect was first discovered in magnetic multilayers,[3] and consists of a very large change in the electrical resistance under an external magnetic field. The observation, in granular solids, of a GMR comparable to the one found in multilayer systems stimulated the study of transport properties in magnetically heterogeneous media, and raised the interest for the prospective applications of granular magnetic systems, which are very easy to produce, and whose microstructure can be modified by a suitable thermal treatment. Usually, heterogeneous thin films are produced by sputtering or coevaporation of immiscible magnetic and nonmagnetic metals. Only recently, granular solids have been also produced by means of other nonequilibrium fabrication processes, such as mechanical alloying[4,5] or melt-spinning.[6-9] The latter method of preparation allows large quantities of bulk granular material to be produced in the form of long, ductile ribbons (few tens of microns thick, few millimeters wide and tens of meters long). Besides the facility and cost of the production, the final geometry of the ribbons could be of interest for practical purposes.

In both multilayered systems and granular solids, the field dependence of resistivity is generally interpreted by the so-called two-current model, based on spin-dependent scattering of conduction electrons essentially at the magnetic/nonmagnetic interfaces and to a lesser extent within the magnetic regions.[10-12] In particular, the resistance of heterogenous alloys is higher when the magnetic moments of neighboring magnetic entities are not aligned (balanced scattering of spin-up and spin-down conduction electrons), and the effect of the magnetic field is to align the magnetic moments, increasing the macroscopic magnetic ordering (preferred scattering of one spin direction, giving rise to a short-circuit effect), and therefore decreasing the resistance of the system.[11] An alternative explanation of the GMR in granular solids, recently proposed by Kim et al.,[13] is based on the interplay between the interfacial potential barrier and the dipole-dipole scattering, without requiring the presence of spin-dependent scattering. All existing theories predict a dependence of the fractional magnetoresistance ($\Delta R/R$) on the square of the reduced magnetization (M/M_s), as a direct consequence of considering the statistical average of equal, noninteracting magnetic moments. Nevertheless, several experimental data have shown a clear deviation from this predicted behavior, which has been explained using a wide variety of arguments. Xiao and co-workers find a deviation from the quadratic law at high fields.[2] Hickey et al. have found that $\Delta R/R$ varies linearly with magnetization in granular $Cu_{100-x}Co_x$, and they ascribe this trend to a wide distribution of Co particles sizes (distribution of blocking temperatures).[14] This alteration of the form of the field dependence of GMR was previously predicted by Zhang and

Levy using a box distribution of particle sizes.[11] Although a distribution of magnetic cluster sizes is not discarded by Bellouard et al.,[15] they point out that other important factors could cause this deviation, such as the alignment of the disordered surface spin under a high magnetic field.[15] The discrepancies found in the literature refer not only to the causes of deviation from the quadratic law, but also to the field region where this deviation occurs. Gregg et al. have found a clear flat-top parabola when plotting the $\Delta R/R$ vs M/M_s curve for Co-Ag at low temperatures, attributing the lack of agreement of the M^2 law at low fields to the presence of different magnetic phases within the sample.[16] Numerical simulations performed by El-Hilo et al. show that interaction effects among the active magnetic regions can explain why at low fields the $\Delta R/R(M^2)$ curve exhibits a flat region.[17]

In order to obtain the best GMR response, the as-produced materials are normally submitted to thermal treatments, in order to precipitate nanometer-sized particles of the magnetic element. In fact, there exist several theories and models trying to quantitatively describe the GMR phenomenon and its dependence upon temperature, magnetic particle sizes and composition.[11,13,18-21] In all existing models one of the most important parameters is the magnetic particle size, which directly determines the spin-dependent scattering through the surface-to-volume ratio and particle distance. These predictions agree with experiments, where an inverse proportionality between the magnetic cluster size and the GMR ratio has been generally observed. However, it is very difficult to account for all factors that can affect the magnetoresistance in granular materials, making the search for an excellent magnetoresistive response somewhat empirical. Therefore, an optimized GMR ratio should result from a proper choice of the material's composition, thermal treatment temperature, and time. A promising alternative to conventional furnace annealing is the use of fast annealing techniques, which have been successfully applied to metastable alloys in order to induce peculiar microstructures with interesting physical properties.[22] In particular, the intrinsic conceptual and practical simplicity of Joule heating techniques allows one to induce a wide range of microstructures in metallic materials, generally displaying improved magnetic and mechanical properties.[23-25]

In this work we perform a detailed and systematic study of the magnetic properties and the GMR effect in rapidly solidified granular $Cu_{100-x}Co_x$ systems ($x=5,10,15$). Melt-spun ribbons of $Cu_{100-x}Co_x$ were submitted to both furnace annealing and dc Joule heating[22] to optimize the GMR response. The distribution of magnetic particle sizes, their spatial density, and mean distance are obtained as functions of the alloy's composition and of the heat treatment by analyzing the anhysteretic magnetization curves measured on the samples at room temperature, as discussed in Sec. IV. The GMR results are plotted as functions of the reduced magnetization. Although all GMR curves exhibit a parabolic dependence on M/M_s at high fields, a significant flattening is observed at low fields (Sec. V). In the case of $Cu_{85}Co_{15}$, such a flattening is very remarkable (the GMR at $M/M_s=0$ is about one-third of the value predicted by extrapolating the parabola fitting the high-field data). In the authors' view, such results point to the existence of a large degree of correlation among magnetic moments. A simple analytical theory of the GMR

in these granular systems, taking explicitly into account the correlation existing among the magnetic particles, is proposed in Sec. VI. According to this theory, the GMR is determined by the ratio of two distinct correlation ranges (one for the angle of tilt of individual magnetic moments with the field axis, the other for the angle of twist of each moment around the same axis) to the electronic mean free path. A generalized expression for the magnetic correlation ranges, independent of the actual coupling energy between moments, is explicitly obtained. A formula describing the magnetic behavior of the GMR is proposed, and shown to accurately fit all the experimental curves.

II. EXPERIMENT

Continuous ribbons of $Cu_{100-x}Co_x$ ($x=5$, 10, and 15 at. %) were obtained by planar flow casting in He atmosphere on a CuZr wheel. The quenching parameters were controlled during the rapid solidification process for all studied compositions in order to get comparable quenching rates.

Different ribbon strips of the three compositions (width 5×10^{-3} m, thickness $4-6\times10^{-5}$ m) were submitted either to conventional furnace annealing in Ar atmosphere at 440 °C for 1 h, or to dc Joule heating in vacuum, in order to induce the precipitation of Co particles. dc Joule heating is a technique of fast annealing, where the heat released to a metallic sample by a constant electrical current is exploited to rapidly increase the sample temperature. In fact, heating rates of the order 10^2-10^3 K/s are routinely obtained.[23] Each sample was clipped between two copper electrodes (length of the sample 0.1 m), and submitted to a direct current (in the range 2 A $\leq I \leq 14$ A) for a fixed time ($t=60$ s). The sample's electrical resistance was determined by measuring the voltage drop across a standard resistor in series with the sample.

Magnetization and magnetoresistance curves were obtained at room temperature on both as-quenched and annealed ribbon strips. The magnetoresistance was measured up $|H|=20$ kOe through a conventional four-contact technique. The magnetic field was applied in the ribbon's plane, perpendicular to the bias current (transverse configuration). Measurements performed with the magnetic field parallel to the ribbon plane indicated that the magnetoresistance in these granular systems is substantially isotropic, as expected.[1,2] The value of the giant magnetoresistance (GMR) for a given value of H was defined as $[(R(H)-R(H=0))/R(H=0)]\times100$.

The magnetic moment of each sample was measured using a vibrating-sample magnetometer VSM (LDJ, model 9500) with an applied field H varying between ±10 kOe. The hysteresis loops were obtained starting from $H=10$ kOe and changing the field intensity by a fixed value (200 Oe). In addition, the corresponding anhysteretic magnetization curves were determined starting from the demagnetized state and gradually increasing the applied field in either direction. In this case, the field was again set to zero after each measurement.

III. RESULTS

The magnetic hysteresis loops of the as-quenched ribbons are reported in Fig. 1 for the studied compositions. All
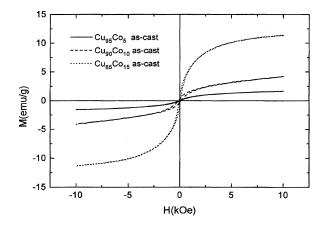
FIG. 1. Magnetic hysteresis loops of as-cast samples of $Cu_{100-x}Co_x$ alloys.

curves display both superparamagnetic and ferromagnetic features. The small area of measured loops and the unsaturating behavior of the curves indicate the presence of a superparamagnetic phase. The ferromagnetic behavior is evidenced by the values of remanence and coercivity, which are indeed rather low (M_r ranges between 0.2 and 1 emu/g, H_c between 10 and 50 Oe), clearly indicating that the starting material is not an ideal solid solution of Co in Cu. It should be noted that the high-field magnetization increases with increasing the Co content.

Figure 2 shows the hysteresis loops of selected samples submitted to different Joule-heating treatments [(a) $Cu_{95}Co_5$, $I=13$ A; (b) $Cu_{90}Co_{10}$, $I=6$ A; (c) $Cu_{85}Co_{15}$, $I=7.5$ A]. These samples displayed the highest GMR values at the maximum applied field (see below). Both the high-field magnetization and the coercive field H_c are observed to increase in these samples with respect to the as-cast ones, indicating both an increased fraction of precipitated Co and a larger mean size of Co clusters (or larger interactions between neighboring particles[26]). However, the hysteresis loops substantially maintain their superparamagnetic features (no tendency towards saturation, and contained loop area).

Figures 3 and 4 show two examples of the close relation-
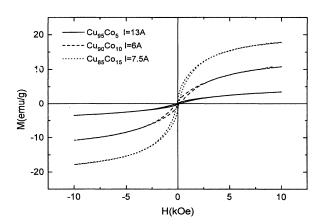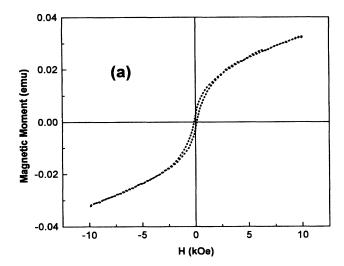

FIG. 2. Magnetic hysteresis loops of $Cu_{100-x}Co_x$ samples exhibiting the best room-temperature magnetoresistance.
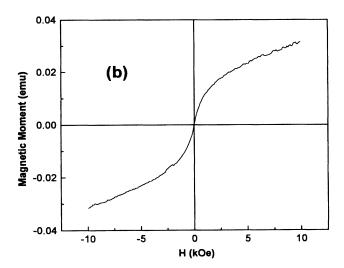

FIG. 3. Room-temperature magnetic moment of an as-cast $Cu_{90}Co_{10}$ sample vs applied field; (a) hysteretic behavior; (b) anhysteretic curve.

ship existing in all studied samples between hysteretic and anhysteretic curves of both magnetization and magnetoresistance. The hysteresis loop and the anhysteretic curve of an as-cast sample of $Cu_{90}Co_{10}$ are plotted in Figs. 3(a) and 3(b). The magnetoresistance curves, measured on a $Cu_{90}Co_{10}$ ribbon strip submitted to a Joule-heating treatment with an electrical current of 6 A for 60 s either on the hysteresis loop (a) and on the anhysteretic curve (b), are reported in Fig. 4. The maximum negative value reached in both cases is approximately the same. The GMR measurement performed on the magnetic hysteresis loop display a hysteretic behavior [see the inset in Fig. 4(a)], because the magnetoresistance is a function of the magnetization rather than of the applied field. The zero value of the GMR is therefore found in correspondence of the coercive field H_c.[2] On the other hand, the electrical resistance variation measured on the anhysteretic curve is symmetric with respect to $H=0$ [see Fig. 4(b)]. Both curves display a nonsaturating behavior of the GMR ratio for high field values, confirming that the alignment of the mag-
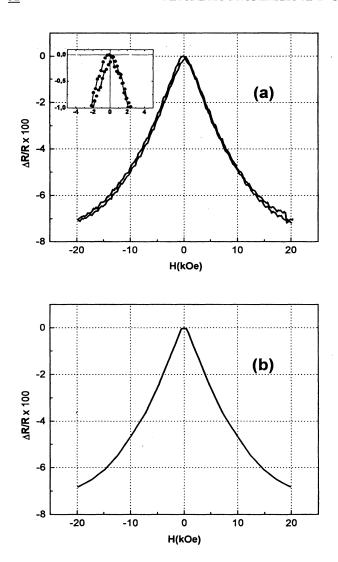
FIG. 4. Room-temperature behavior of the giant magnetoresistance of a Joule-heated $Cu_{90}Co_{10}$ alloy ($I=6$ A, $t=60$ s) as a function of the magnetic field; (a) hysteretic behavior; (b) anhysteretic curve.
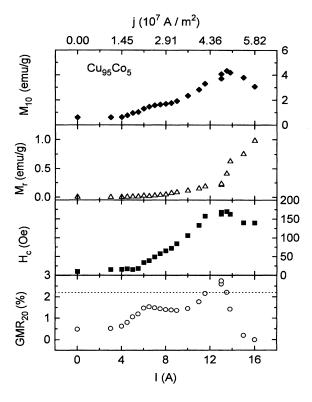

FIG. 5. Effect of Joule heating under different electrical currents on representative magnetic and electric parameters (defined in the text) of the $Cu_{95}Co_5$ alloy. Joule-heating time: 60 s. Dashed line: best GMR_{20} value exhibited by the conventionally annealed material.

netic moments can only be reached for applied fields much higher than 20 kOe.

Figures 5–7 summarize the behavior of the electrical and magnetic properties routinely measured on samples of all examined compositions, submitted to different electrical current densities j. The magnetization at $H=10$ kOe (M_{10}), the magnetic remanence (M_r), the coercive field (H_c) are reported together with the magnetoresistance value at $H=20$ kOe (GMR_{20}). For low j values ($j<2.5\times10^7$, 1.4×10^7, 1.5×10^7 A/m^2 for $Cu_{95}Co_5$, $Cu_{90}Co_{10}$, $Cu_{85}Co_{15}$, respectively) the magnetoresistance remains almost the same as in the as-cast alloys. In addition, the magnetic parameters are nearly constant, or slightly increasing, indicating that no significant changes in the number and size of the as-quenched magnetic clusters has occurred. In the intermediate region of j values ($2.5\times10^7<j<4.8\times10^7$ A/m^2, $1.4\times10^7<j<2\times10^7$ A/m^2, $1.5\times10^7<j<2.5\times10^7$ A/m^2 for $Cu_{95}Co_5$, $Cu_{90}Co_{10}$, $Cu_{85}Co_{15}$, respectively), GMR_{20} significantly increases up to

a maximum value (2.75%, 7.1%, 6.9% in $Cu_{95}Co_5$, $Cu_{90}Co_{10}$, $Cu_{85}Co_{15}$, respectively). Correspondingly, M_{10} increases, indicating the precipitation of magnetic particles. On the other hand, in $Cu_{90}Co_{10}$ and $Cu_{85}Co_{15}$, both the remanence M_r and the coercive field H_c remain nearly constant, indicating a persistent superparamagnetic behavior of the treated materials. The constant value of H_c provides a clue that Joule-heating treatments are effective in inducing the nucleation of particles of size comparable with the as-quenched ones, rather than the growth of preexisting magnetic nuclei. In $Cu_{95}Co_5$, H_c is observed to steadily increase until j reaches the value j_{opt} corresponding to the peak of GMR_{20}, staying almost constant for $j>j_{opt}$. The region of high j values is characterized by a monotonic decrease of GMR_{20}, while the magnetization M_{10} is observed to stay constant, or even to slightly decrease with j. In $Cu_{90}Co_{10}$ and $Cu_{85}Co_{15}$, both the coercive field and the remanence display a significant increase, possibly indicating a process of growth of magnetic clusters. It should be noted that the conventionally annealed samples exhibit lower maxima of GMR_{20} (2.2%, 4.7%, 3.8% for $Cu_{95}Co_5$, $Cu_{90}Co_{10}$, $Cu_{85}Co_{15}$ furnace annealed for 1 h at 440 °C, respectively: see horizontal dotted lines in Figs. 5–7).

The reduction in M_{10} observed in $Cu_{95}Co_5$ and $Cu_{85}Co_{15}$ above j_{opt} may indicate that some Co is redissolved in the Cu matrix, according to a mechanism postulated by Wecker et al., and expected to act at high temperatures.[6] Actually,
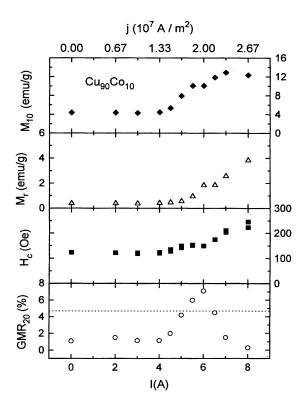
FIG. 6. Same as in Fig. 5 for the $Cu_{90}Co_{10}$ alloy.

FIG. 7. Same as in Fig. 5 for the $Cu_{85}Co_{15}$ alloy.

such an effect has been observed by us in samples submitted to high values of the electrical-current density.

IV. PARTICLE SIZE ANALYSIS

A model based on the coexistence of superparamagnetic and ferromagnetic particles has been recently exploited to explain the magnetic behavior of similar granular systems.[27] The magnetization curve is viewed as the superposition of a suitable Langevin function and an *ad hoc* analytical function describing a hysteretic contribution of given coercivity and squareness. In principle, such a model could be applied to the present case also, in order to determine the average size of superparamagnetic particles (from the Langevin function) and the one of ferromagnetic particles (from H_c). As known, the measured coercivity is often assumed to provide a good estimate of the size of fine particles above the so-called critical diameter for the appearance of superparamagnetism.[28] However, in the present case, different evidences point to a substantial inadequacy of this procedure to determine the particle size.

(1) The critical diameter for superparamagnetism is not exactly known, because it depends on the value of the dominant magnetic anisotropy energy in Co particles. The latter could originate either from the particle's crystalline structure, or from their shape. The magnetic anisotropy energy could range in this case from about 4×10^5 erg/cm^3 for spherical particles of fcc Co, to 2×10^6 erg/cm^3 for slightly elongated particles of fcc Co, to 4×10^6 erg/cm^3 for spherical particles of hcp Co,[28] leading to a room-temperature critical diameter for superparamagnetism of 17, 10, 7.6 nm, respectively.

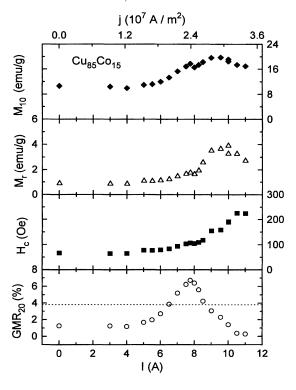(2) In addition, the low coercivity of the assembly of Co

particles may be explained (a) by assuming the presence of clusters of size larger than the critical size; (b) by invoking the presence of interactions between particles whose size may be smaller than the critical size.[26]

(3) The measured hysteresis loops always look like broadened Langevin functions, and are rather poorly fitted by a superposition of a Langevin function and of a hysteretic magnetization curve (either of the type used by Stearns and Cheng,[27] or the one describing the magnetic behavior of an assembly of ferromagnetic particles, according, e.g., to the Stoner's model[28]).

The experimental evidence leads us to introduce a different approach to the study of the size distribution of Co clusters in the considered systems. From this viewpoint, more information can be extracted from the overall shape of the magnetization curves than from the coercivity values. As a consequence, the anhysteretic magnetization curves, whose correspondence to the hysteresis loops is always apparent (see Fig. 3) may be proposed as the most convenient data to be analyzed in terms of Langevin functions. It should be explicitly noted that the superparamagnetic character of an assembly of fine particles is just a matter of the time scale of the experiments performed to determine their magnetic behavior.[28] In principle, therefore, the hysteresis loops measured on the considered samples should reduce to the corresponding anhysteretic curves by merely performing magnetic measurements on a longer time scale.

In the present case, the Co grains dispersed in the Cu matrix are assumed to be independent and distributed in size. The rather simplified picture approximation of independent superparamagnetic particles (see next section) is a suitable starting point to analyze the particle-size distribution.[6,29] The
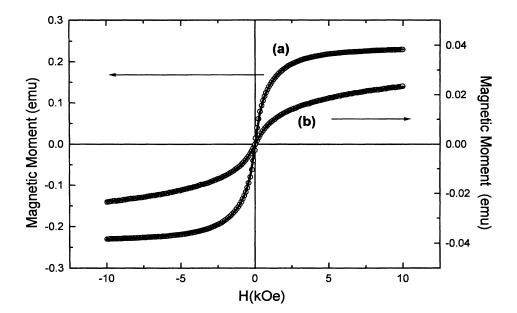
FIG. 8. Anhysteretic behavior of the magnetic moment of two representative samples of the $Cu_{100-x}Co_x$ family. Circles: experimental data; full lines: best fit according to Eq. (1). (a) Joule-heated $Cu_{85}Co_{15}$, $I=9$ A, $t=60$ s; (b) as-cast $Cu_{95}Co_5$.

Langevin function depends on the grain size through the particle's magnetic moment. In fact, the measured anhysteretic curves of all samples are never described by a single Langevin function. The experimental data are instead well described in terms of a weighted sum of few Langevin functions, each describing the contribution to the resulting magnetic moment of a set of clusters of given size. Shorthand information about the structure of the studied granular materials can be therefore obtained through an analysis of this type, completely based upon magnetic data. The fitting function is therefore of the form

$$M = M_0 \sum_i p_i \mathscr{L}_i(d_i), \tag{1}$$

where $\mathscr{L}_i$ is the Langevin function, M_0 and d_i are the alloy's magnetization and particle diameter, respectively, and the weights p_i satisfy the conditions $\sum_i p_i = 1$ and $p_i \geq 0$.

In the present analysis, the diameter of Co particles was assumed to be distributed in the range 2–7.5 nm, in agreement with the results reported in the literature.[1,12,30] The fits appeared to be systematically worsened by using diameter values exceeding both limits. The number of Langevin curves entering the fitting function was a compromise between the contrasting requirements of increasing the resolution of this analysis, and of providing reliable and stable values of the p_i's. The best results were obtained using four Langevin functions in Eq. (1). In this case the d_i's ($i=1,4$) take the values 2.5, 4.2, 5.8, 7.5 nm. The fits obtained through Eq. (1) on a Joule-heated $Cu_{85}Co_{15}$ sample ($I=9$ A, curve a) and an as-cast $Cu_{95}Co_5$ sample (curve b) are shown in Fig. 8 as examples of the validity of such a procedure. The agreement is excellent in all cases. The present analysis was exploited in samples submitted to different thermal treatments (either Joule heating or conventional annealing) in order to get information on the evolution of Co clusters. It should be noted that the observation of small Co particles through x-ray diffraction or electrical microscopy is difficult

owing to the inherent difficulty in separating the contributions of Cu and Co, which are characterized by closely similar lattice parameters.[31]

Typical results obtained by using this technique of analysis are summarized in Figs. 9–11 for $Cu_{95}Co_5$, $Cu_{90}Co_{10}$, $Cu_{85}Co_{15}$, respectively. The normalized particle-size frequency is shown in Figs. 9–11 (top). The density of Co particles of a given size, N_i, was obtained by multiplying the weights p_i by the total number of particles per unit volume, N, obtained from the equation:

$$N\bar{\mu} = M_s^*, \tag{2}$$

where M_s^* is the alloy's saturation magnetization, and $\bar{\mu}$ is the average magnetic moment

$$\bar{\mu} = \sum_i p_i \left(\frac{\pi}{6} d_i^3\right) M_s^{(Co)}, \tag{3}$$

$M_s^{(Co)}$ being the saturation magnetization of bulk Co. As a consequence,

$$N_i = N p_i = \frac{M_s^* p_i}{\bar{\mu}} = \frac{p_i}{\frac{\pi}{6} \sum_i p_i d_i^3} \frac{M_s^*}{M_s^{(Co)}}. \tag{4}$$

The value of M_s^* is determined by extrapolating the fitting function of Eq. (2) to $H \to \infty$. The N_i values are reported in Figs. 9–11 (bottom).

The histograms shown in Figs. 9–11 include, for each composition, the as-quenched ribbon, three Joule-heated samples and the high-GMR_{20} samples obtained by conventional annealing ($T_a = 440$ °C for 1 h). The Joule-heated samples of $Cu_{90}Co_{10}$ and $Cu_{85}Co_{15}$ were selected in order to show the changes in cluster-size distribution in the ribbon submitted to the optimum electrical current density for GMR (j_{opt}), and in two ribbons where j was respectively lower and higher than j_{opt}. In the case of $Cu_{95}Co_5$, the sample with maximum GMR was compared with two ribbons submitted
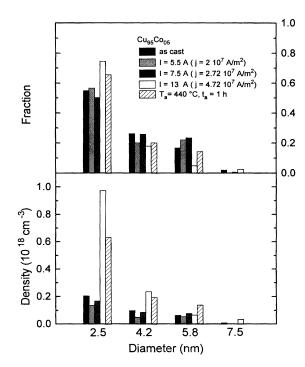
FIG. 9. Histograms showing the normalized fraction (above) and the density (below) of Co particles of given mean diameter for the $Cu_{95}Co_5$ alloy system.

to electrical current densities lower than j_{opt}, and characterized by rather different values of H_c (20 and 50 Oe).

Generally speaking, the heat treatments induce a moderate shift in the average cluster size towards higher values. The density of very small magnetic particles ($d=2.5$ and 4.2 nm)
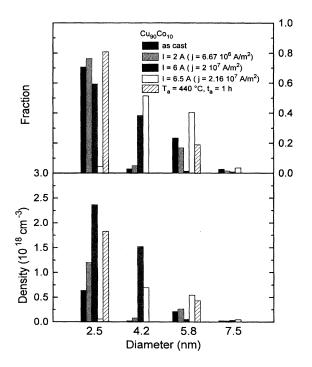

FIG. 10. Same as in Fig. 9 for the $Cu_{90}Co_{10}$ alloy system.
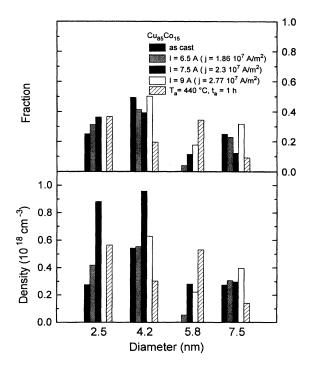

FIG. 11. Same as in Fig. 9 for the $Cu_{85}Co_{15}$ alloy system.

is always the highest in materials displaying the maximum GMR. However, comparing high-GMR systems obtained by furnace annealing and Joule heating, one finds that the latter is more effective in producing a high density of small clusters, and a slightly lower density of large particles. The nominal alloy's composition plays a relevant role too: the integrated density of magnetic clusters increases with increasing the percentage of Co in the alloy's composition. However, the maximum density of very small grains ($d=2.5$ and 4.2 nm), found in samples displaying the highest GMR value, is 1.2×10^{18} cm^{-3} in $Cu_{95}Co_5$, about 4×10^{18} cm^{-3} in $Cu_{90}Co_{10}$, about 1.9×10^{18} cm^{-3} in $Cu_{85}Co_{15}$. Finally, the reduction in GMR for electrical current density values beyond j_{opt} appears to be related to a strong reduction in the number of the smallest grains ($d=2.5$ nm), clearly observed in $Cu_{90}Co_{10}$ and in $Cu_{85}Co_{15}$. These materials exhibit a significant fraction of magnetic particles having larger diameters, possibly indicating a process of growth of preexisting grains. The present analysis may explain why Joule heating turns out to be more effective in enhancing the GMR value.

Samples of different nominal compositions submitted to different electrical current densities were characterized by markedly different values of the total particle density, N. The role of N on the room-temperature magnetoresistance is clearly shown in Fig. 12(a), where GMR_{20} is plotted against N. The same data are plotted in Fig. 12(b) against the mean intergranular distance a, defined through the relation $\mathcal{N} a^3 = V$, or $Na^3 = 1$, $\mathcal{N}$ being the total number of particles contained in the volume V. It can be concluded that the highest GMR is found in materials where a great number of relatively small and densely packed Co clusters may develop. From this viewpoint, the $Cu_{95}Co_5$ alloy is not particularly suitable, because the Co clusters, although properly small, cannot reach a high density. On the other hand, $Cu_{90}Co_{10}$ and
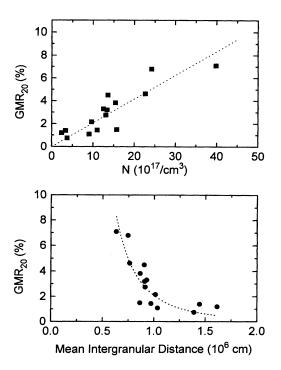
FIG. 12. Dependence of GMR_{20} on the total density of magnetic particles (above) and on the mean intergranular distance (below) for the $Cu_{100-x}Co_x$ family. The dotted lines are guides for the eye.

$Cu_{85}Co_{15}$ show similar GMR maxima, although N is markedly different in these samples (4×10^{18} and 2.4×10^{18} cm^{-3}, respectively). Such a fluctuation (and, more generally, the scattering of data in Fig. 12) clearly indicates that N is only one of the parameters affecting the GMR, which is obviously influenced by other factors, involving the electrical properties of the material, such as the ratio between the average intergranular distance, a, and the electronic mean free path.[27]

Finally, a comment about the grain sizes obtained through the present analysis is needed. In all cases, the anhysteretic curves are definitely not fitted by admitting the existence of particles having larger sizes ($d \geq 8$ nm). It should be noted that all reported size distributions rapidly tail off in their right sides, indicating that the particle diameter is rather small in the majority of cases. This outcome is in line with other findings on similar alloy systems.[1,12] In light of these results, the appearance of a nonzero coercivity may indicate either that the critical size for superparamagnetism is in the range 7–8 nm, or that the Co clusters cannot be considered as independent. The first explanation is compatible with a high magnetic anisotropy of Co particles, like the one associated to hcp Co, or (more probably Ref. 31) to elongated particles of fcc Co. However, relevant magnetic interactions among Co clusters are always present in the considered systems, as the analysis of the next section will show beyond any doubt.

V. EVIDENCE FOR MAGNETIC INTERACTIONS AMONG Co PARTICLES

A close relationship exists in bimetallic granular systems between the alloy's magnetoresistance and the global mag-

netization. General arguments show that the GMR must be an even function of the reduced magnetization $m = M/M_s^*$, where M_s^* is the saturation magnetization.[10–13] A well-established and particularly simple approach makes use of plots of the GMR as a function of m^2.[2,16] In fact, the variation of the alloy's resistivity with the degree of field-induced magnetic order may be simply pictured as[32]

$$\rho = \rho_0 - k \frac{\langle [\mu_i \cdot \mu_j]^{(\lambda)} \rangle}{\mu^2} = \rho_0 - k \langle \cos \theta_{ij}^{(\lambda)} \rangle, \qquad (5)$$

where ρ_0 and k are constants and $\langle [\mu_i \mu_j]^{(\lambda)} \rangle = \mu^2 \langle \cos \theta_{ij}^{(\lambda)} \rangle$ is the value (averaged over the whole material) of the scalar product between magnetic moments (assumed to have equal magnitude, for the sake of simplicity) at a distance r_{ij} apart. Such a distance must not exceed by large amounts the electronic mean free path λ.[27] In the considered systems, the room-temperature mean free path is typically of the order of the average distance between adjacent particles.[27]

Usually, the expectation value of $\cos \theta_{ij}^{(\lambda)}$ is assumed to be

$$\langle \cos \theta_{ij}^{(\lambda)} \rangle = \langle \cos \theta_i \rangle \langle \cos \theta_j \rangle = m^2, \qquad (6)$$

where θ_i is the angle between μ_i and the field axis. This result holds in the case of complete lack of correlation among the angles θ_i in the material.[2,16] As a consequence, $\Delta R/R \equiv \Delta \rho/\rho$ is predicted to be written (in the simplest case) as

$$\frac{\Delta R}{R} = -\frac{k}{\rho_0} \langle \cos \theta_{ij}^{(\lambda)} \rangle = -\left(\frac{k}{\rho_0} \right) m^2. \qquad (7)$$

In some cases, a quadratic dependence of $\Delta R/R$ on m^2 is actually found.[2,16] Deviations from such a behavior in the low-m region are, however, not unusual, and are often mentioned as a proof of the existence of magnetic interactions among particles.[16]

In this section, we apply such an analysis to our measurements. The reduced magnetization value used to plot GMR as a function of m was obtained from the magnetization measured on the anhysteretic curve, divided by a saturation value, determined by extrapolating the previously determined fitting function [Eq. (1)] to $H \rightarrow \infty$. In fact, the distinctly superparamagnetic behavior of the considered materials implies that the highest measured magnetization value (M_{10}) is not an accurate approximation of M_s^*.

Let us generalize Eq. (7) by admitting that $\langle \cos \theta_{ij}^{(\lambda)} \rangle$ may be nonzero when $H = 0$, as expected in the presence of correlation among magnetic moments.[16] In this case, $\Delta R/R$ should be written as

$$\frac{\Delta R}{R} = \frac{k[\langle \cos \theta_{ij}^{(\lambda)} \rangle_0 - \langle \cos \theta_{ij}^{(\lambda)} \rangle]}{\rho_0 - k \langle \cos \theta_{ij}^{(\lambda)} \rangle_0}, \qquad (8)$$

where $\langle \cos \theta_{ij}^{(\lambda)} \rangle_0 = \langle \cos \theta_{ij}^{(\lambda)} \rangle|_{H=0}$. The denominator in Eq. (8) is always greater than zero. In the limit of very large H, i.e., when $|m| \rightarrow 1$, the correlation among magnetic moments becomes negligible,[16,33] so that $\langle \cos \theta_{ij}^{(\lambda)} \rangle|_{|m| \rightarrow 1} \rightarrow m^2$. As a consequence, Eq. (8) reduces to a parabola in the limit $|m| \rightarrow 1$:

$$\left.\frac{\Delta R}{R}\right|_{m=\pm 1} = \frac{k\langle\cos\theta_{ij}^{(\lambda)}\rangle_0}{\rho_0 - k\langle\cos\theta_{ij}^{(\lambda)}\rangle_0} - \frac{1}{\rho_0 - k\langle\cos\theta_{ij}^{(\lambda)}\rangle_0}m^2$$

$$= a - bm^2. \qquad (9)$$

The quantities a, b are obtained by fitting the tails at large m of the $\Delta R/R$ curve to a parabola of the type $f(m) = a - bm^2$. The reduced GMR is then defined as

$$\left(\frac{\Delta R}{R}\right)_{\text{red}} = \frac{\frac{\Delta R}{R} - f(m=1)}{f(m=0) - f(m=1)} = \frac{\frac{\Delta R}{R} - a + b}{b}$$

$$= 1 - \langle\cos\theta_{ij}^{(\lambda)}\rangle. \qquad (10)$$

In the absence of correlation, $(\Delta R/R)_{\text{red}}$ should behave as $1 - m^2$, as expected. Otherwise, $(\Delta R/R)_{\text{red}}$ should characteristically flatten out around $m = 0$, owing to the fact that $\langle\cos\theta_{ij}^{(\lambda)}\rangle_0$ is nonzero in a correlated magnetic system. A strong flattening of $(\Delta R/R)_{\text{red}}$ in proximity of $m = 0$ is actually found in all studied systems, as shown in Figs. 13–15, where the curves of three representative samples of each composition are reported. This result, found in all examined cases, gives strong evidence to the hypothesis of correlation among magnetic moments. The value of the reduced GMR at $m = 0$ may be taken as a shorthand measure of the degree of deviation of the system from the behavior of an assembly of independent magnetic moments. The $(\Delta R/R)_{\text{red}}$ curves are very flat in the case of $Cu_{85}Co_{15}$, apparently indicating that the magnetic moments are rather strongly correlated. Quite interestingly, all curves become more parabolic after sample heating. Such a behavior is seemingly conflicting with the fact that sample heating increases the density and size of magnetic clusters, as discussed above. This result may however be explained on the basis of a simplified theory where the hypothesis of correlation among magnetic moments is explicitly worked out.

VI. A SIMPLE THEORY OF GMR IN CORRELATED SUPERPARAMAGNETIC SYSTEMS

A. General framework

In the present approach, all magnetic moments are supposed to be equal in size (μ) and randomly scattered within the material, with average nearest-neighbor distance a. The central parameter in this approach is the average value of $\cos\theta_{ij}$. Introducing the angle of tilt θ_i between each magnetic moment and the field axis (z axis), and the angle of twist ϕ_i measuring the azimuth in the (x, y) plane, and admitting that θ_i and ϕ_i are independent stochastic variables, $\langle\cos\theta_{ij}\rangle$ may be written as

$$\langle\cos\theta_{ij}\rangle = \langle\cos\theta_i \cos\theta_j\rangle + \langle\sin\theta_i \sin\theta_j\rangle\langle\cos(\phi_i - \phi_j)\rangle.$$

$$(11)$$

Usually, the hypothesis of complete lack of correlation between twist angles of any pair of magnetic moments is made, so that $\langle\cos(\phi_i - \phi_j)\rangle = 0$. As a consequence, $\langle\cos\theta_{ij}\rangle$ reduces to $\langle\cos\theta_i \cos\theta_j\rangle$, i.e., to m^2 if the additional hypothesis of lack of correlation between tilt angles is made. On the other hand, if all magnetic moments were parallel, $\langle\cos\theta_{ij}\rangle$ would
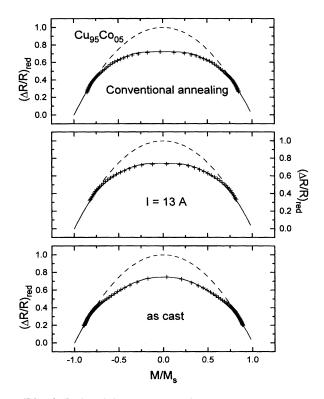

FIG. 13. Reduced GMR curves as functions of reduced magnetization for three selected samples of $Cu_{95}Co_5$. Crosses: experimental data; dashed lines: parabolic behavior predicted by the independent-moment model; full lines: present model [Eq. (28)]. A reduced number of experimental data is displayed. The fits were performed on the whole set of data.

be equal to unity, independent of the value of the applied field. In that case, according to Eq. (10), $(\Delta R/R)_{\text{red}}$ would always be zero.

In paramagnetic systems, the twist angles of adjacent moments are supposed to be completely uncorrelated, owing to the dominant effect of the stochastic torque of thermal origin acting on each moment. In the present case, however, the interaction energy between moments is no more negligible with respect to kT. In fact, by using the data of Table I, the ratio μ^2/a^3, which gives an order-of-magnitude estimate of the energy per moment arising from either dipolar or Ruderman-Kittel-Kasuya-Yosida (RKKY) interaction, is not much smaller than kT, particularly at high Co concentrations.

In order to phenomenologically describe this correlation, a field dependent, twist-angle correlation length $r_\phi(H)$ may be introduced:

$$\langle\cos(\phi_i - \phi_j)\rangle = e^{-[r_{ij}/r_\phi(H)]}, \qquad (12)$$

where r_{ij} is the distance between moments i and j, so that $\langle\cos\theta_{ij}\rangle$ is written as

$$\langle\cos\theta_{ij}\rangle = \langle\bar{u}_i\bar{u}_j\rangle + \langle(1 - \bar{u}_i)^{1/2}(1 - \bar{u}_j)^{1/2}\rangle e^{-[r_{ij}/r_\phi(H)]}, \qquad (13)$$

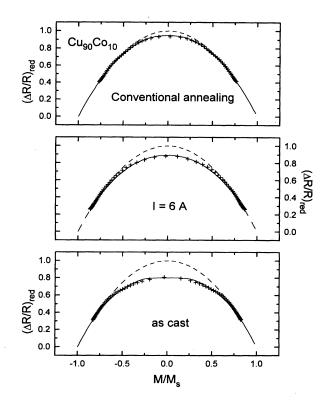where $\bar{u}_i = \cos\theta_i$ is a space-dependent stochastic variable,

FIG. 14. Same as in Fig. 13 for $Cu_{90}Co_{10}$.

FIG. 15. Same as in Fig. 13 for $Cu_{85}Co_{15}$.

whose meaning is explained by considering that the fairly large values of μ found in the considered systems allow one to use classical arguments to discuss the dynamics of a magnetic moment submitted to a magnetic field (either applied, or of internal origin). In fact, any moment tendentially performs a precession around the field direction, with a fixed tilt angle θ_i. A stochastic torque of thermal origin acts to interrupt the time coherence of the moment's precession, so that both $\theta_i(t)$ and $\phi_i(t)$ are randomly varying with time. The quantity $\bar{u}_i$ appearing in Eq. (13) is obtained by averaging
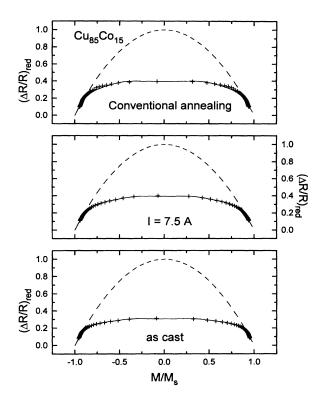
$u_i(t) = \cos\theta_i(t)$ over times much longer than the coherence time of the moment's precession.

Let us explicitly introduce the internal field acting on site i:

$$H_i = \mu \sum_k \lambda_{ik}\bar{u}_k, \tag{14}$$

where the coupling constants λ_{ik} describe the total interaction between moments, and may take positive as well as

TABLE I. Average magnetic moment, mean intergranular distance, ratio of the magnetic to thermal energy, and correlation parameter for the GMR of all studied $Cu_{100-x}Co_x$ alloys.

Sample	μ (emu)	distance a (cm)	$\mu^2/(a^3kT)$	$(\mu^2/a^3)^{1/2}R_{ac}/R_{ann}$
$Cu_{85}Co_{15}$, as cast	1.06×10^{-16}	9.70×10^{-7}	0.310	1.11×10^{-7}
$Cu_{85}Co_{15}$, $I=6.5$ A	1.02×10^{-16}	9.09×10^{-7}	0.345	7.40×10^{-8}
$Cu_{85}Co_{15}$, $I=7.5$ A	7.94×10^{-17}	7.46×10^{-7}	0.379	5.54×10^{-8}
$Cu_{85}Co_{15}$, $I=9$ A	1.50×10^{-16}	9.30×10^{-7}	0.700	6.02×10^{-8}
$Cu_{85}Co_{15}$ (1 h, 440 °C)	9.25×10^{-17}	8.67×10^{-7}	0.329	4.36×10^{-8}
$Cu_{90}Co_{10}$, as cast	5.21×10^{-17}	1.04×10^{-6}	0.061	4.95×10^{-8}
$Cu_{90}Co_{10}$, $I=2$ A	4.07×10^{-17}	8.62×10^{-7}	0.065	5.09×10^{-8}
$Cu_{90}Co_{10}$, $I=6$ A	3.19×10^{-17}	6.32×10^{-7}	0.100	3.49×10^{-8}
$Cu_{90}Co_{10}$, $I=6.5$ A	9.71×10^{-17}	9.05×10^{-7}	0.318	4.85×10^{-8}
$Cu_{90}Co_{10}$ (1 h, 440 °C)	3.68×10^{-17}	7.63×10^{-7}	0.076	1.71×10^{-8}
$Cu_{95}Co_{05}$, as cast	5.06×10^{-17}	1.39×10^{-6}	0.024	3.08×10^{-8}
$Cu_{95}Co_{05}$, $I=5.5$ A	4.94×10^{-17}	1.61×10^{-6}	0.014	2.07×10^{-8}
$Cu_{95}Co_{05}$, $I=7.5$ A	5.50×10^{-17}	1.44×10^{-6}	0.025	2.32×10^{-8}
$Cu_{95}Co_{05}$, $I=13$ A	3.31×10^{-17}	9.16×10^{-7}	0.035	1.70×10^{-8}
$Cu_{95}Co_{05}$ (1 h, 440 °C)	3.87×10^{-17}	1.01×10^{-6}	0.036	1.10×10^{-8}

negative values. The summation in Eq. (14) is not intended to be performed over first neighbors only. It should be noted that Eq. (14) represents, as usual, the z component of the field $\mathbf{H}_i$, whose fluctuating transverse components are supposed to be averaged out on the considered time scale. As a consequence

$$\bar{u}_i = \mathscr{L}\left[\frac{\mu(H+H_i)}{kT}\right] = \mathscr{L}\left[\frac{\mu H + \mu^2 \Sigma_k \lambda_{ik}\bar{u}_k}{kT}\right], \quad (15)$$

where $\mathscr{L}$ is the Langevin function. The magnetic interaction among moments must be weak, because these systems are not magnetically ordered at room temperature. The magnetic ordering temperature predicted by the theory is $T_c = (\mu^2 \langle \Sigma_k \lambda_{ik} \rangle)/(3k)$. It should be noted that for purely dipolar interactions among moments, either arranged on a cubic lattice, or randomly distributed in space, $\Sigma_k \lambda_{ik}$ is rigorously equal to zero for each site i,[33] so that T_c would be zero in that case. By developing Eq. (15) up to the first order in the perturbative term $\mu^2 \Sigma_k \lambda_{ik}\bar{u}_{ik}/kT$, one gets

$$\bar{u}_i = \bar{u} + \delta_i, \quad (16)$$

where $\bar{u}$ is the implicit solution of the equation

$$\bar{u} = \mathscr{L}\left[\frac{\mu H + \mu^2 \langle \Sigma_k \lambda_{ik} \rangle \bar{u}}{kT}\right] \quad (17)$$

and δ_i is a site-dependent fluctuation defined as

$$\delta_i = \frac{\mu^2}{kT} \mathscr{L}'\left[\frac{\mu H + \mu^2 \langle \Sigma_k \lambda_{ik} \rangle \bar{u}}{kT}\right] \sum_k \lambda_{ik}\delta_k. \quad (18)$$

The fluctuation δ_i on site i is therefore linearly dependent on similar fluctuations on neighboring sites. The function $\mathscr{L}'$ in Eq. (18) is the first derivative of $\mathscr{L}$ (x) with respect to x. Since T_c is very small when compared to T, the quantity $\bar{u}$ may be written as $\bar{u} = \mathscr{L}(\mu H/kT)$ without introducing any substantial error. By defining the quantity $S_i = \Sigma_k \lambda_{ik}\delta_k$, it becomes possible to introduce a field-dependent tilt-angle correlation length $r_\theta(H)$ through the expression

$$\langle S_i S_j \rangle = \langle S_i^2 \rangle e^{-[r_{ij}/r_\theta(H)]}, \quad (19)$$

the average value $\langle S_i \rangle$ being zero. The quantities $\langle \bar{u}_i \bar{u}_j \rangle$ and $\langle (1 - \bar{u}_i^2)^{1/2}(1 - \bar{u}_j^2)^{1/2} \rangle$ appearing in Eq. (13) may be evaluated with the help of Eq. (16) and by developing the square roots of the type $(1 - \bar{u}_i^2)^{1/2}$ up to the second order in the small parameters S_i's. The final expression for $\langle \cos \theta_{ij} \rangle$ turns out to be

$$\langle \cos\theta_{ij} \rangle = \bar{u}^2 + (\langle u^2 \rangle - \bar{u}^2)e^{-[r_{ij}/r_\theta(H)]} + \left[1 - \bar{u}^2 - \frac{\langle u^2 \rangle - \bar{u}^2}{1 - \bar{u}^2}(1 - \bar{u}^2 e^{-[r_{ij}/r_\theta(H)]})\right]e^{-[r_{ij}/r_\phi(H)]}, \quad (20)$$

where $\bar{u} \equiv m$ and $\langle u^2 \rangle = 1 - 2[\mathscr{L}(\mu H/kT)/(\mu H/kT)]$. When $H=0$, $\bar{u}_0 = 0$, $\langle u^2 \rangle_0 = 1/3$. The ratio $(\langle u^2 \rangle - \bar{u}^2)/(1 - \bar{u}^2)$ is not diverging when $\bar{u} \to \pm 1$. Let us evaluate the behavior of $\langle \cos\theta_{ij} \rangle$ with m in two limiting cases: (a) absence of both tilt- and twist-angle correlation between moments i and j $(r_{ij} \gg r_\theta, r_{ij} \gg r_\phi)$: $\langle \cos\theta_{ij} \rangle = m^2$; (b) complete correlation of both tilt and twist angle, i.e., parallel moments $(r_{ij} \ll r_\theta, r_{ij} \ll r_\phi)$: $\langle \cos\theta_{ij} \rangle = 1$.

B. Field dependence of the correlation ranges

It should be noted that both r_θ and r_ϕ must be decreasing functions of H, because the degree of correlation between any two moments must decrease with increasing H.[33] The tilt-angle correlation length r_θ may be given an explicit functional dependence on H through the following argument. Let us introduce a system where all moments are ideally aligned: $\bar{u}_j = \bar{u}$. Now, let us introduce a fluctuation on the site i at a distance r_i from the origin: $\bar{u}_i = \bar{u} + \delta_i$. According to Eq. (18), such a fluctuation induces a disturbance on the neighboring moments, giving rise to a fluctuation field. Admitting that the fluctuation is smoothly varying with distance, any δ_k may be written in terms of δ_i as

$$\delta_k = \delta_i + \left[\left(\frac{\partial\delta}{\partial x}\right)_i x_{ik} + \left(\frac{\partial\delta}{\partial y}\right)_i y_{ik} + \left(\frac{\partial\delta}{\partial z}\right)_i z_{ik}\right]$$
$$+ \frac{1}{2}\left[\left(\frac{\partial^2\delta}{\partial x^2}\right)_i x_{ik}^2 + \cdots\right] + \cdots, \quad (21)$$

where x_{ik}, y_{ik}, z_{ik} are the components of $\mathbf{r}_{ik}$. As a consequence, Eq. (18) transforms to

$$\delta_i \approx \frac{\mu^2}{kT}\mathscr{L}'\left[\frac{\mu H}{kT}\right]\left[\left(\sum_k \lambda_{ik}\right)\delta_i + \left(\sum_k \lambda_{ik}x_{ik}\right)\left(\frac{\partial\delta}{\partial x}\right)_i + \cdots\right.$$
$$\left. + \frac{1}{2}\left(\sum_k \lambda_{ik}x_{ik}^2\right)\left(\frac{\partial^2\delta}{\partial x^2}\right)_i + \cdots\right], \quad (22)$$

where the argument of $\mathscr{L}'$ has been simplified neglecting $[\mu^2 \langle \Sigma_k \lambda_{ik} \rangle \bar{u}]$ with respect to μH, as previously discussed. For the same reasons, it may be assumed that $\Sigma_k \lambda_{ik} \approx 0$ for any site i (this term should vanish in the presence of a purely dipolar interaction among randomly distributed moments). In addition, terms of the type $\Sigma_k \lambda_{ik}x_{ik}$ may be shown to be substantially zero, admitting that λ_{ik} is sufficiently long ranged and dependent on r_{ik} only. In fact, in an assembly of

randomly distributed moments, the probability of finding a moment at a distance r_{ik} from i is equal to the one of finding a moment at a distance r_{ik}. The only surviving terms in the development (22) are therefore those containing sums of the type $\Sigma_k \lambda_{ik} x^2_{ik}$. In isotropic systems,

$$\sum_k \lambda_{ik} x^2_{ik} = \sum_k \lambda_{ik} y^2_{ik} = \sum_k \lambda_{ik} z^2_{ik} = \alpha. \qquad (23)$$

The constant α is positive in systems where the coupling is predominantly of ferromagnetic or dipolar type. In the continuum approximation, Eq. (22) transforms to

$$\Delta \delta(r) = \cfrac{1}{\cfrac{\mu^2}{kT} \mathscr{L}'\left(\cfrac{\mu H}{kT}\right) \alpha} \delta(r) \equiv \frac{1}{r^2_\theta(H)} \delta(r), \qquad (24)$$

where Δ is the Laplacian operator. Equation (24) admits a solution of the type

$$\delta(r) \approx \frac{e^{-[r/r_\theta(H)]}}{r}, \qquad (25)$$

where r must be larger than the average distance between neighboring moments, a. The quantity r_θ, defined as

$$r_\theta(H) = \left[\frac{\mu^2}{kT} \alpha \mathscr{L}'\left(\frac{\mu H}{kT}\right)\right]^{1/2} = \sqrt{3} r_\theta(0) \left[\mathscr{L}'\left(\frac{\mu H}{kT}\right)\right]^{1/2} \qquad (26)$$

plays the role of a correlation range for the angle of tilt. This quantity decreases monotonically with increasing H, as expected. The maximum value of $r_\theta, r_\theta(0)$, depends not only on the temperature and the μ value, but also on the nature on the interaction among moments (through the parameter α).

A comment on the role of the twist-angle correlation length and on its behavior with H is required. Totally neglecting the twist-angle correlation (as generally done in the existing approaches) implies that the minimum value of $\langle \cos\theta_{ij} \rangle$ should never be lower than $\langle \cos\theta_{ij} \rangle_0 \equiv \langle u^2 \rangle_0 = 1/3$, according to Eq. (20). In that case, $[(\Delta R/R)_{\text{red}}]_{H=0}$ expressed by Eq. (10) should not be lower than $1 - \langle u^2 \rangle_0 = 2/3 = 0.667$ (corresponding to complete correlation of twist angles). Generally speaking, all experimental values of the quantity $[(\Delta R/R)_{\text{red}}]_{H=0}$ determined on $Cu_{95}Co_{05}$ and $Cu_{90}Co_{10}$ alloys are systematically higher than 0.667 (see Figs. 13 and 14). However, $[(\Delta R/R)_{\text{red}}]_{H=0}$ is definitely lower than 2/3 in $Cu_{85}Co_{15}$ alloys, as shown in Fig. 15. From our viewpoint, this result unequivocally points to the existence of an instantaneous correlation between twist angles of adjacent moments. Let us explicitly note that in $Cu_{85}Co_{15}$ alloys the interaction energy of dipolar origin, roughly equal to μ^2/a^3, and responsible for a tendency towards persistent alignment of adjacent moments, is no more negligible with respect to kT, as remarked before (see Table I).

Obviously, the theory developed in the previous subsection cannot be applied to get information on the twist-angle correlation and r_ϕ. In fact, that approach was based upon the study of the site-dependent fluctuation of the expectation value $\bar{u}_i$, obtained performing a time average of the stochastic quantity $u_i(t)$ over a time interval much longer than the time of moment's precession around the z axis. In order to correctly explore the tilt-angle correlation, one should inves-

tigate the much more complex dynamics of interacting pairs of magnetic moments on a much shorter time scale. In this paper, such a problem is not dealt with, in view of its intrinsic difficulty and of the lack of substantial information about the nature of the dominant interaction between moments. As a consequence, we make the simplifying hypothesis that r_ϕ depends on H according to a law formally similar to the one derived for r_θ [Eq. (26)], i.e.,

$$r_\phi(H) = \sqrt{3} r_\phi(0) \left[\mathscr{L}'\left(\frac{\mu H}{kT}\right)\right]^{1/2}, \qquad (27)$$

where the maximum value $r_\phi(0)$ is left as a free parameter, to be determined from a fitting procedure.

C. Comparison with experimental data

Making use of Eq. (20), the term $\langle \cos\theta_{ij}^{(\lambda)} \rangle$ appearing in the expression for $(\Delta R/R)_{\text{red}}$ [Eq. (10)] may be suitably approximated by

$$\langle \cos\theta_{ij}^{(\lambda)} \rangle = \bar{u}^2 + (\langle u^2 \rangle - \bar{u}^2) e^{-[\lambda/r_\theta(H)]}$$

$$+ \left[1 - \bar{u}^2 - \frac{\langle u^2 \rangle - \bar{u}^2}{1 - \bar{u}^2} (1 - \bar{u}^2 e^{-[\lambda/r_\theta(H)]})\right]$$

$$\times e^{-[\lambda/r_\phi(H)]}, \qquad (28)$$

where λ is the room-temperature electronic mean free path. The reduced GMR is therefore determined, in this simple approach, by the ratio between the correlation ranges (for both tilt and twist angles) and the electronic mean free path.

The $(\Delta R/R)_{\text{red}}$ curves of Figs. 13–15 are fitted through Eq. (10) and Eq. (28). The results are shown in the same figures. The same excellent agreement is observed in all examined alloys. The only free parameters in these fits are the values of $r_\theta(0)/\lambda$ and $r_\phi(0)/\lambda$. A map of the values of these parameters for the $Cu_{100-x}Co_x$ system is obtained by plotting $r_\phi(0)/\lambda$ against $r_\theta(0)/\lambda$ (see Fig. 16). Generally speaking, the correlation ranges of both tilt and twist angles are larger than λ, with only two exceptions. In addition, the tilt-angle correlation appears to be slightly more extended in space than the twist-angle correlation, which is, however, always present. In the low-correlation limit, both correlation lengths become equal. Obviously, the $Cu_{85}Co_{15}$ family is characterized by the highest values of both $r_\theta(0)/\lambda$ and $r_\phi(0)/\lambda$, as expected. The full lines in Fig. 16 represent the loci of all pairs of $r_\theta(0)/\lambda$ and $r_\phi(0)/\lambda$ values giving rise to the same flattening of the $(\Delta R/R)_{\text{red}}$ curve. It should be stressed, however, that all choices of these paired parameters, other than the ones shown in Fig. 16, lead to a mismatch between theoretical curves and experimental data.

The variation in λ with respect to the as-cast materials may be obtained checking the changes induced by heat treatment on the electrical resistance R. The ratio between the effective electronic mean free path in annealed and as-cast samples may be expressed as $(\lambda_{\text{ann}}/\lambda_{\text{ac}}) = (R_{\text{ac}}/R_{\text{ann}})$. This ratio is reported in Table I for all studied alloys. On the other hand, $r_\theta(0)$ is proportional to $(\mu^2\alpha)^{1/2}$ [see Eq. (26)]. With dipolar or RKKY interactions among moments, $\alpha \approx 1/a^3$, so that $r_\theta(0) \approx (\mu^2/a^3)^{1/2}$. The quantity $[(\mu^2/a^3)^{1/2} R_{\text{ann}}/R_{\text{ac}}]$, which may be termed as the correlation parameter for the GMR and is reported in Table I, provides a figure of the
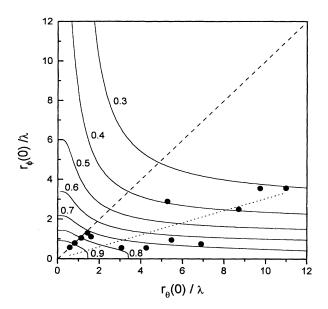
FIG. 16. Map of the ratios between the maximum values of tilt- and twist-angle correlation ranges $[r_\theta(0), r_\phi(0)]$ and the electronic mean free path λ, as deduced by the best fit of the experimental $(\Delta R/R)_{\text{red}}$ curves (full circles). Full lines: loci of the pairs of $r_\theta(0)/\lambda$, $r_\phi(0)/\lambda$ values giving rise to the same flattening of $(\Delta R/R)_{\text{red}}$ (as indicated). Dashed line: locus of the points corresponding to equal magnetic ranges. The dotted line is a guide for the eye.

overall effect of annealing on the ratio $r_\theta(0)/\lambda$. Quite interestingly, such a ratio is observed to decrease with annealing. Such a result explains why the experimental $(\Delta R/R)_{\text{red}}$ curves become definitely more parabolic after annealing. Finally, it should be noted that in all studied alloy systems, the samples exhibiting the highest GMR_{20} values are characterized by the smallest values of the quantity $[(\mu^2/a^3)^{1/2} R_{\text{ann}}/R_{\text{ac}}] \approx r_\theta(0)/\lambda$. This feature emphasizes once more the substantial role played by the ratio between magnetic correlation ranges and electronic mean free path in determining the intensity of the GMR effect in these systems.

VII. CONCLUDING REMARKS

The present results, concerning the magnetic properties and the GMR effect of the $Cu_{100-x}Co_x$ alloy system, allow us to draw definite conclusions about the magnetic structure of these granular materials.

First, the Co particle sizes appear to be distributed in a relatively narrow interval of diameters, even in annealed alloys. The effect of further annealing, presumably leading to a generalized growth of magnetic particles, has not been studied.

The Joule-heating technique always provides slightly higher values of GMR than conventional annealing. This outcome may be connected to the superior aptitude of Joule heating in generating very small Co particles.

These results were obtained through a rather simplified analysis, based on the assumption of independent magnetic moments. A more detailed study shows that the moments on neighboring Co particles are indeed correlated, owing to the presence of competing, long-range magnetic interactions (presumably either of dipolar or RKKY type). Although the systems are magnetically disordered at room temperature, a rather strong correlation among moment fluctuations is to be expected.

As a consequence, the weights of Co particles of a given size, p_i, provided in Sec. IV, should be considered as merely indicative. A model interpreting both the hysteresis loops and the anhysteretic magnetization curves of these materials in terms of an ordering of weakly interacting magnetic moments is, however, still lacking. In our opinion, the overall information about grain sizes and their changes, as emerging from the analysis of Sec. IV, is substantially correct and unequivocal, if viewed as a first approximation of a more accurate picture of the physical system.

Two correlation ranges, respectively for the angle of tilt of the magnetic moments with respect to the field axis, and for their angle of twist around the same axis, are needed to correctly account for the flattening of the GMR vs m^2 curves and for their overall shapes. These magnetic correlation ranges are not independent of each other; they simultaneously increase or decrease, depending on the alloy's composition.

A relevant role on the absolute value of GMR, and on the shape of the $(\Delta R/R)_{\text{red}}$ curves, is played by the ratio of the magnetic correlation ranges to the electronic mean free path.

On the light of these results, the naive picture of a granular magnetic alloy as an essentially superparamagnetic system characterized by a single parameter measuring the field-induced magnetic order (the angle of tilt between moments and the field axis) has to be discarded. A more correct approach to the problem should take into account the full short-time dynamics of magnetic moments and their instantaneous angles of tilt and twist. Such an approach is needed because the characteristic duration of the coherent moments' precession around the field axis is not negligible with respect to the time of flight of electrons between adjacent magnetic scatterers.

[1] A. E. Berkowitz, J. R. Mitchell, M. J. Carey, A. P. Young, S. Zhang, F. E. Spada, F. T. Parker, A. Hutten, and G. Thomas, Phys. Rev. Lett. **68**, 3745 (1992).

[2] J. Q. Xiao, J. S. Jiang, and C. L. Chien, Phys. Rev. Lett. **68**, 3749 (1992).

[3] M. N. Baibich, J. M. Broto, A. Fert, F. Nguyen van Dau, F. Petroff, P. Etienne, G. Creuzet, A. Friederich, and J. Chazeles, Phys. Rev. Lett. **61**, 2472 (1988).

[4] A. R. Yavari, P. J. Desré, and T. Benameur, Phys. Rev. Lett. **68**, 2235 (1992).

[5] J. G. Cabañas Moreno, V. M. Lopez, H. A. Calderon, and J. C. Rendon-Angeles, Scr. Metall. Mater. **28**, 645 (1993).

[6] J. Wecker, R. von Helmolt, L. Schultz, and K. Samwer, Appl. Phys. Lett. **62**, 1985 (1993); IEEE Trans. Magn. **29**, 3087 (1993).

[7] B. Dieny, A. Chamberod, C. Cowache, J. B. Genin, S. R. Teixeira, R. Ferre, and B. Barbara, J. Magn. Magn. Mater. **135**, 191 (1994).

[8] M. El Ghannami, C. Gómez-Polo, G. Rivero, and A. Hernando, Europhys. Lett. **26**, 701 (1994).

[9] P. Allia, C. Beatrice, M. Knobel, P. Tiberto, and F. Vinai, J. Appl. Phys. **76**, 6817 (1994).

[10] S. Zhang, Appl. Phys. Lett. **61**, 1855 (1992).

[11] S. Zhang and P. M. Levy, J. Appl. Phys. **73**, 5315 (1993).

[12] T. A. Rabedeau, M. F. Toney, R. F. Marks, S. S. P. Parkin, R. F. C. Farrow, and G. R. Harp, Phys. Rev. B **48**, 16 810 (1993).

[13] J. H. Kim, J. Q. Xiao, C. L. Chien, and Z. Tesanovic, Solid State Commun. **89**, 157 (1994).

[14] B. J. Hickey, M. A. Howson, S. O. Musa, and N. Wiser, Phys. Rev. B **51**, 667 (1995).

[15] C. Bellouard, B. George, and G. Marchal, J. Phys. Condens. Matter **6**, 7239 (1994).

[16] J. F. Gregg, S. M. Thompson, S. J. Dawson, K. Ounadjela, C. R. Staddon, J. Hamman, C. Fermon, G. Saux, and K. O'Grady, Phys. Rev. B **49**, 1064 (1994).

[17] M. El-Hilo, K. O'Grady, and R. W. Chantrell, J. Appl. Phys. **76**, 6811 (1994).

[18] M. Rubinstein, Phys. Rev. B **50**, 3830 (1994).

[19] Y. Asano, A. Oguri, J. Inoue, and S. Maekawa, Phys. Rev. B **49**, 12 831 (1994).

[20] J.-Q. Wang and G. Xiao, Phys. Rev. B **49**, 3982 (1994).

[21] D. J. Kubinski and H. Holloway, J. Appl. Phys. **77**, 2508 (1995).

[22] P. Allia, M. Baricco, P. Tiberto, and F. Vinai, Phys. Rev. B **47**, 3118 (1993).

[23] P. Allia, M. Baricco, P. Tiberto, and F. Vinai, Rev. Sci. Instrum. **64**, 1053 (1993).

[24] P. Allia, M. Baricco, M. Knobel, P. Tiberto, and F. Vinai, J. Magn. Magn. Mater. **133**, 243 (1994).

[25] P. Allia, M. Baricco, M. Knobel, P. Tiberto, and F. Vinai, J. Magn. Magn. Mater. **140–144**, 617 (1995).

[26] D. V. Berkov and S. V. Meshkov, IEEE Trans. Magn. **26**, 1804 (1990).

[27] M. B. Stearns and Y. Cheng, J. Appl. Phys. **75**, 6894 (1994).

[28] B. D. Cullity, *Introduction to Magnetic Materials* (Addison-Wesley, Reading, MA, 1972), passim.

[29] Chubing Peng and Daosheng Dai, J. Appl. Phys. **76**, 2986 (1994).

[30] M. A. Howson, S. O. Musa, M. J. Walker, B. J. Hicley, R. Cochrane, and R. Stevens, J. Appl. Phys. **75**, 6546 (1994).

[31] A. Hütten and G. Thomas, Ultramicroscopy **52**, 581 (1993).

[32] M. R. Parker, J. A. Barnard, D. Seale, and A. Waknis, J. Appl. Phys. **73**, 5512 (1993).

[33] A. Herpin, *Théorie du Magnétisme* (Presses Universitaires de France, Paris, 1968), p. 294.